Available online at www.sciencedirect.com
ScienceDirect
Journal of Magnetic Resonance 192 (2008) 151–158
JMR Journal of Magnetic Resonance
www.elsevier.com/locate/jmr

# Sources of sensitivity losses in ultrafast 2D NMR

Patrick Giraudeau *, Serge Akoka

*Université de Nantes, Nantes Atlantique Universités, CNRS, Laboratoire d'Analyse Isotopique et Electrochimique de Métabolismes, UMR 6006, Faculté des Sciences, B.P. 92208, 2 rue de la Houssinière, F-44322 Nantes Cedex 03, France*

Received 21 December 2007; revised 4 February 2008
Available online 14 February 2008

**Abstract**

Recent ultrafast techniques make it possible to obtain *n*D NMR spectra in a single scan. However, an important sensitivity decrease is observed when the excitation duration is increased, which is necessary to improve resolution. A detailed, theoretical and experimental study of sensitivity losses in ultrafast experiments is carried out on the example of *J*-resolved spectroscopy. The importance of molecular diffusion effects during both encoding and acquisition phases is shown by numerical simulations and experimental results. Other possible sources of signal-to-noise decrease are also considered, such as transverse relaxation, homonuclear *J*-couplings or chemical shift effects.


*Keywords:* Ultrafast 2D NMR; *J*-resolved spectroscopy; Sensitivity; Molecular diffusion; Homonuclear couplings

## 1. Introduction

Two-dimensional Nuclear Magnetic Resonance (2D NMR) [1,2] is a powerful analytical tool used in a wide range of applications, from the study of chemical structures and dynamics to pharmaceutical and medical applications. However, it suffers from long acquisition times due to the necessary collection of numerous $t_1$ increments to obtain spectra with a good resolution.

Recently, a method based on ultrafast imaging techniques was proposed by Frydman and co-workers [3,4], allowing the acquisition of 2D NMR spectra within a single scan. In this so-called "ultrafast 2D NMR" technique, the usual $t_1$ encoding was initially replaced by a discrete spatial encoding, followed by a detection block based on Echo Planar Imaging (EPI) [5]. However, this discrete encoding suffered from several drawbacks which led to its replacement by a continuous encoding scheme [6], using a pair of continuously frequency-swept pulses applied during a bipolar gradient. Unfortunately, this method involves an amplitude modulation which is incompatible with phase-modulated techniques such as COSY [1] or *J*-resolved spectroscopy [7]. Three different alternatives were then proposed [8–10] to obtain a phase-modulated encoding in order to circumvent these limitations. Tal's encoding scheme [8] consists of a 90° continuous excitation performed by a chirp pulse with a linear frequency ramp applied during a positive gradient, immediately followed by a 180° chirp pulse applied during a positive gradient. A slightly different version of Tal's encoding pattern was suggested by Andersen and Kockenberger [9], in which the second gradient is reversed. Finally, Pelupessy proposed a double spin echo method [10] starting with a 90° non-selective pulse, followed by a pair of identical 180° chirp pulses applied during alternated gradients. Based on these continuous phase-modulated excitation schemes, we have proposed [11] a modification of the acquisition scheme to obtain *J*-resolved spectra where coupling constants are encoded along the direct $v_2$ domain. In a recent paper [12], we showed that when resolution in the ultrafast dimension is improved by increasing the duration $T_e$ of the excitation pattern, dramatic sensitivity losses and intensity distortions are observed. Molecular diffusion appeared to be the main cause of signal-to-noise ratio decrease, but its effects were not studied in details.

* Corresponding author. Fax: +33 (0)2 51 12 57 12.
*E-mail address:* patrick.giraudeau@univ-nantes.fr (P. Giraudeau).

1090-7807/$ - see front matter © 2008 Elsevier Inc. All rights reserved.
doi:10.1016/j.jmr.2008.02.007

In this paper, a thorough, theoretical and experimental quantitative study of sensitivity losses in ultrafast experiments is carried out. Diffusion effects during both encoding and acquisition phases are carefully analyzed by numerical simulations and experimental results. Other possible sources of sensitivity losses are also considered, such as transverse relaxation, homonuclear *J*-couplings or chemical shift offset effects.

## 2. Results and discussion

In order to evaluate the various sources of sensitivity losses, our recently developed ultrafast *J*-resolved scheme [11] was applied to a model compound (100 mM ethyl acetate sample in DMSO-$d_6$) presenting various *J*-coupling patterns. Its ultrafast 2D *J*-resolved spectrum is presented on Fig. 1 together with the corresponding pulse sequence, based on Pelupessy's continuous phase-encoding scheme [10]. In the following study, Pelupessy's encoding scheme and Tal's scheme with inverted gradient (as described in [12]) will be considered, as they were shown to have the same efficiency concerning resolution aspects [12].

### 2.1. Sensitivity losses during encoding period

In a previous study [12], dramatic signal-to-noise losses were observed when increasing the average time $T_e$ spent by magnetizations in the transverse plane, which is defined in [12] for each excitation scheme. Fig. 2 shows the evolution of ethyl acetate peak intensities as a function of $T_e$ for Pelupessy's scheme. In order to compare signals under similar conditions, intensities were determined in separate experiments for the three peaks. In each case, the excitation frequency was set on the relevant signal in order to cancel chemical shift offset effects. Moreover, each observed peak was set in the middle of the acquisition window to make sure that signals are compared under the same acquisition conditions (see Section 2.2). A dramatic intensity decrease is observed when $T_e$ increases, with similar evolutions for each of the three peaks, which confirms the results obtained in Ref. [12]. Experiments performed using Tal's excitation scheme with inverted gradient show the same evolution with even more important sensitivity decrease. This evolution may *a priori* originate from various sources such as transverse relaxation, molecular diffusion or homonuclear *J*-coupling modulations.

We measured the transverse relaxation times of ethyl acetate, and the following values were obtained: 0.9 s for the quadruplet at 4.05 ppm, 4.6 s for the singlet at 2.00 ppm and 3.6 s for the triplet at 1.19 ppm. These values are much higher than the duration of the excitation period, which limits the influence of transverse relaxation. The maximum magnetization decrease due to relaxation at the end of a 180 ms encoding period would be 18% for the quadruplet, 4% for the singlet and 5% for the triplet. Regarding the intensity decrease observed on Fig. 2 for $T_e = 180$ ms (53–59%), it is clearly demonstrated that transverse relaxation is not the main cause of sensitivity losses.

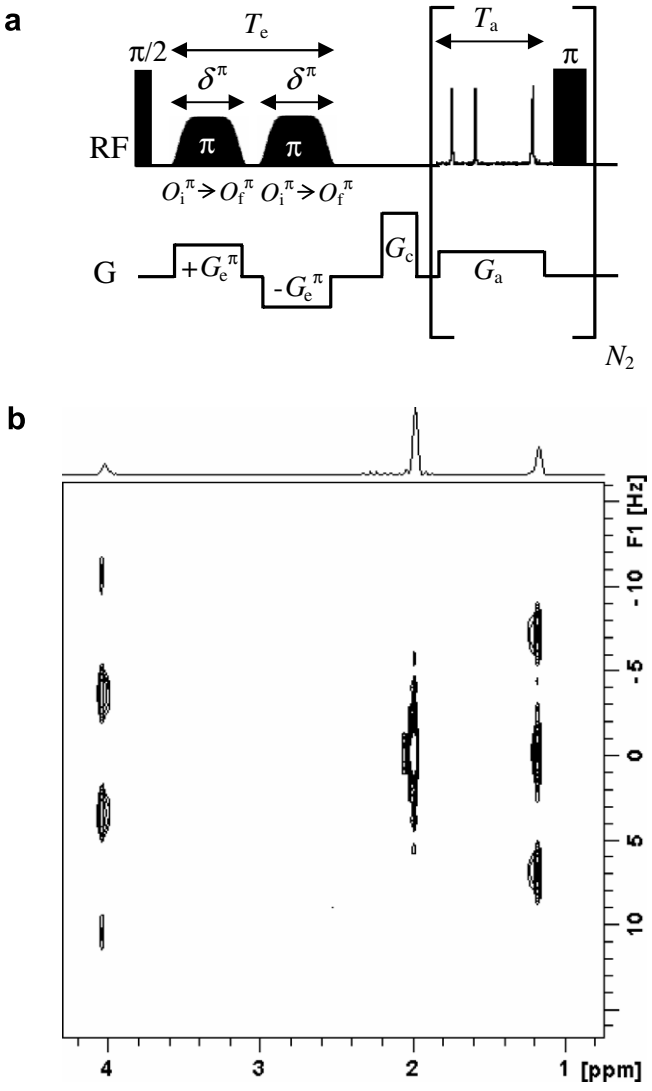


Fig. 1. (a) Pulse sequence for the acquisition of ultrafast 2D *J*-resolved spectra, using the phase-modulated encoding scheme proposed by Pelupessy. The $G_c$ gradient prior to acquisition is adjusted to set the middle of the chemical shift range in the middle of the detection period $T_a$. The 180° pulse phase is alternated ($y$, $y$, $-y$, $-y$) to avoid undesirable stimulated echoes. (b) Ultrafast 500 MHz *J*-resolved spectrum acquired in 500 ms on a 100-mmol $L^{-1}$ ethyl acetate sample in DMSO-$d_6$ at 303 K, using the above pulse sequence with $T_e = 60$ ms.

In several papers [8,10], molecular diffusion was supposed to be responsible for sensitivity losses in continuous encoding ultrafast experiments, but to our knowledge, its effects were never studied in a quantitative way. They are quite easy to understand if we remember that for two gradient pulses placed on each side of a 180° pulse, the intensity $I$ of the observed signal, observed as a fraction of the signal intensity in the absence of a gradient, $I_0$ is given by [13]:

$$\frac{I}{I_0} = \exp(-b \cdot D) \tag{1}$$

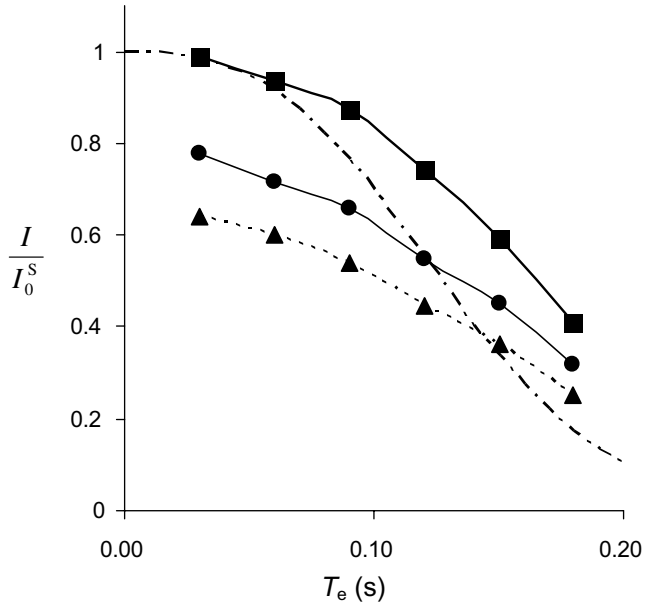


Fig. 2. Influence of the excitation period duration $T_e$ on peak intensity for ultrafast $J$-resolved spectra of a 100-mmol $L^{-1}$ ethyl acetate sample in DMSO-$d_6$, for the singlet at 2.00 ppm (—■—), for the triplet at 1.19 ppm (—●—) and for the quadruplet at 4.05 ppm (- - -▲- - -). The simulated curve (-.-.-.) for the singlet at 2.00 ppm is also represented. In order to compare intensities with equal dependence to diffusion and offset effects, measurements were performed on separate experiments for each signal. Each peak was set in the middle of the acquisition window and the excitation frequency was set on the relevant signal. Average intensities for three consecutive experiments are plotted relatively to the singlet peak intensity for $T_e \approx 0$. Intensities were divided by the number of corresponding protons.

where $b$ is a function of the amplitude and duration of the gradient pulses, also depending on the time between the onset of the two gradients. $D$ is the self-diffusion constant. In the case of Pelupessy's scheme, we shall call $\tau^{\pi}(\Omega_1, z)$ the instant when the first chirp pulse addresses an internal chemical shift $\Omega_1$ at a particular $z$ position [8]. This instant $\tau^{\pi}$ is given by

$$\tau^{\pi}(\Omega_1, z) = \frac{\Omega_1 - O_i^{\pi} + \gamma_e G_e^{\pi} z}{R^{\pi}} \tag{2}$$

where $O_i^{\pi}$ is the initial frequency offset of the chirp pulse characterized by a sweep rate $R^{\pi}$, and $G_e^{\pi}$ is the amplitude of the encoding gradient. It can be shown (cf. Appendix A) that the diffusion factor $b_{Pel}$ for the whole excitation scheme is given by

$$b_{Pel} = \frac{2}{3}\gamma^2 \left(G_e^{\pi}\right)^2 \left[(\tau^{\pi})^3 + (\delta^{\pi} - \tau^{\pi})^3\right] \tag{3}$$

where $\delta^{\pi}$ is the duration of the 180° chirp pulse. In this model, gradient decay and build-up times are not considered, as they are very short compared to $\delta^{\pi}$. For comparison, a similar analysis can be carried out in the case of Tal's scheme with inverted gradient. As an example, we studied the case where the duration $\delta^{\pi/2}$ of the 90° chirp pulse is twice the duration $\delta^{\pi}$ of the 180° chirp pulse. As indicated by Eq. (7) in Ref. [8], it is required that both gradients have the same amplitude ($G_e^{\pi} = -G_e^{\pi/2}$). The corresponding diffusion factor $b_{Tal}$ is given by (cf. Appendix A)

$$b_{Tal} = \frac{1}{3}\gamma^2 \left(G_e^{\pi/2}\right)^2 \left[\left(\delta^{\pi/2} - \tau^{\pi/2}\right)^3 + \left(\frac{\delta^{\pi/2}}{2} - \frac{\tau^{\pi/2}}{2}\right)^3 + \left(\frac{\tau^{\pi/2}}{2}\right)^3 + \left(\frac{\delta^{\pi/2}}{2}\right)^3\right] \tag{4}$$

where $\tau^{\pi/2}(\Omega_1, z)$ is the instant when the first chirp pulse a ddresses an internal chemical shift $\Omega_1$ at a particular $z$ position [8]. This instant $\tau^{\pi/2}$ is given by

$$\tau^{\pi/2}(\Omega_1, z) = \frac{\Omega_1 - O_i^{\pi/2} + \gamma_e G_e^{\pi/2} z}{R^{\pi/2}} \tag{5}$$

where $O_i^{\pi/2}$ is the initial frequency offset of the chirp pulse characterized by a sweep rate $R^{\pi/2}$.

Starting from Eqs. (3) and (4), we calculated signal losses due to diffusion effects for various $z$ coordinates, for a given chemical shift $\Omega_1$. We performed simulations for both Pelupessy and Tal's schemes, for different $T_e$ values. The results are presented on Fig. 3, for a diffusion coefficient $D = 1.0 \times 10^{-9} m^2 s^{-1}$ corresponding to the experimental value for the ethyl acetate sample (see Section 4). It can be observed that diffusion losses during excitation highly depend on the position $z$. Moreover, diffusion losses

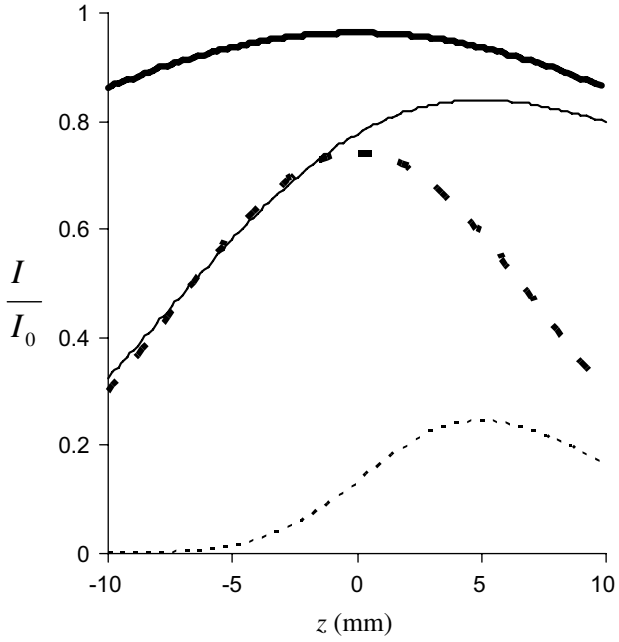


Fig. 3. Simulation of signal losses due to diffusion during excitation, for ultrafast spectra acquired with Pelupessy's encoding scheme [10] (▬ for $T_e = 60$ ms and ▪ ▪ ▪ for $T_e = 120$ ms) and with Tal's encoding scheme with inverted gradient [8,9] (— for $T_e = 60$ ms and - - - - - - for $T_e = 120$ ms). Simulations are performed for 0.011 T $m^{-1}$ excitation gradients and for a diffusion coefficient $D = 1.0 \times 10^{-9}$ $m^2$ $s^{-1}$. Curves obtained at zero frequency are represented, but simulations performed at different frequencies show that diffusion losses do not vary significantly over the $^1$H chemical shift range. Transverse relaxation was not considered in this model.

increase at high $T_e$, which confirms the experimental results. Symmetrical profiles are obtained for Pelupessy's excitation scheme, probably due to the symmetric nature of the encoding scheme, whereas it is not the case for Tal's. Simulations are shown for $\Omega_1 = 0$, but results obtained for different $\Omega_1$ values show that the intensity profile does not vary significantly over the usual $^1$H chemical shift range, because it is much lower than the frequency dispersion induced by the excitation gradients. It demonstrates that chemical shift offset effects are not predominant in continuous encoding ultrafast experiments.

Starting from these simulations, we can calculate the average attenuation at the end of the excitation period over the whole sample, which will determine the intensity decrease for 2D peaks. This attenuation is plotted on Fig. 4 as a function of $T_e$ for both encoding schemes and for two different diffusion coefficients, corresponding to the ethyl acetate sample ($D = 1.0 \times 10^{-9}$m$^2$ s$^{-1}$) and to a 100 mmol L$^{-1}$ 3-ethyl bromopropionate sample in $CDCl_3$ ($D = 1.7 \times 10^{-9}$m$^2$ s$^{-1}$). The curve profile obtained for ethyl acetate is similar to the experimental one (Fig. 2). For comparison, the theoretical curve for the singlet at 2.00 ppm was reported on Fig. 2 after taking into account the effect of transverse relaxation by multiplying the theoretical curve by $e^{-t/T_2}$. Similar evolutions are observed for both experimental and theoretical curves, even though the theoretical model seems to overestimate intensity losses. This difference may be due to experimental errors in the measurement of diffusion coefficients or transverse relaxation times. The simulated results obtained for 3-ethyl bromopropionate (Fig. 4) confirm that intensity losses depend on the diffusion coefficient $D$. Finally, the simulations show that Tal's scheme is more sensitive to diffusion effects than Pelupessy's, which corroborates the experimental results. Moreover, Pelupessy's excitation pattern is easier to implement in routine procedures [12], consequently the following experiments will focus on this encoding scheme.

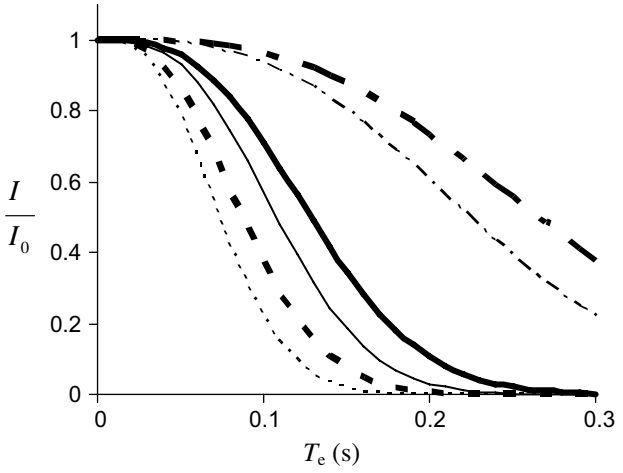


Fig. 4. Simulation of average signal losses due to diffusion during excitation, for ultrafast spectra acquired with Pelupessy's encoding scheme [10] (▬ for $D = 1.0\ 10^{-9}$ m$^2$ s$^{-1}$ and ── for $D = 1.7 \times 10^{-9}$ m$^2$ s$^{-1}$), with Tal's encoding scheme with inverted gradient [8,9] (▬ ▪ ▬ for $D = 1.0 \times 10^{-9}$ m$^2$ s$^{-1}$ and for $D = 1.7 \times 10^{-9}$ m$^2$ s$^{-1}$) and with the multi-echo scheme for $2n = 6$ echoes (–.– for $D = 1.0 \times 10^{-9}$ m$^2$ s$^{-1}$ and for $D = 1.7 \times 10^{-9}$ m$^2$ s$^{-1}$). Simulations are performed for 0.011 T m$^{-1}$ excitation gradients. Curves obtained at zero frequency are represented, but simulations performed at different frequencies show that diffusion losses do not vary significantly over the $^1$H chemical shift range. Transverse relaxation was not considered in this model.

The aforementioned results highlight the influence of molecular diffusion effects. However, another usual source of sensitivity modulation in 2D NMR experiments is the effect of homonuclear $J$-couplings. Their influence on the ultrafast encoding process should also be considered, as it was never addressed before. To evaluate it, we calculated the phase evolution during the encoding process for different multiplets characterized by a coupling constant $J$. As an example, at the end of the two-pulse excitation process, the phase for each component of a doublet is given by

$$\phi_P^0 = \frac{2 \cdot T_e}{L} \cdot \Omega_1 z \pm \pi \cdot J \cdot T_e \tag{6}$$

Similar expressions can be obtained for other coupling patterns. In this expression, it can be noticed that there is no $J \cdot z$ term, consequently $J$-couplings do not affect the spatial encoding constant $C$. This result confirms the experimental curves (Fig. 1) where it can be observed that multiplets undergo the same intensity decrease as the singlet when increasing $T_e$. The constant relative intensity difference observed between the three signals is the same as the one observed on a conventional $J$-resolved spectrum acquired under similar conditions (result not shown). This is due to the well-known effect of $J$-couplings on 2D $J$-resolved peak volume [14] that originates here from the conventional dimension of our ultrafast experiments.

Eq. (6) also reveals an interesting feature of ultrafast $J$-resolved spectroscopy based on Pelupessy's scheme [11]. As the phase at the end of the encoding process does not include any $J \cdot z$ term, signal position in the $k/v_1$ dimension is not affected by coupling constants. In other words, homonuclear-decoupled spectra can be obtained in a single scan without any post-FT processing such as the common tilt operation, thus providing a solution to a recurrent problem in $^1$H NMR spectroscopy. This can be checked on the experimental spectrum (Fig. 1), where the multiplets appear aligned along $v_2$ axis. It is not the case for Tal's encoding scheme, as shown in Ref. [8].

The aforementioned results show that molecular diffusion is the main source of sensitivity decrease during the encoding process, as $J$-couplings have no influence and because relaxation and chemical shift effects do not affect peak intensity in a significant manner. Diffusion effects were studied on $J$-resolved spectra but can be generalized to any ultrafast 2D-pulse sequence based on continuous phase-encoding, as they do not depend on the following mixing or acquisition periods. The first conceivable solution to limit diffusion losses is to use weaker gradient amplitudes. However, the results presented above were

already obtained with the smallest amplitude available on our spectrometer (2% of maximum strength), and lower values would lead to important signal distortions. Another solution is to use the multi-echo encoding scheme recently proposed in [12]. In this pulse sequence based on Pelupessy's technique [10], the two 180° chirp pulses are replaced by a succession of shorter 180° pulse pairs applied during alternated gradients. The duration of 180° pulses is given by $T_e/(2n)$, where $2n$ is the number of echoes. For identical $T_e$ values, theoretical spatial encoding level and resolution are the same as in Pelupessy's scheme, but diffusion effects are reduced because shorter gradients are employed. To check this assessment, we simulated the intensity losses due to diffusion for a $2{\cdot}n = 6$ echo excitation, by applying Eq. (3) three times successively. A symmetrical $z$-dependence of the intensity losses is obtained, as the multi-echo scheme is based on Pelupessy's excitation pattern. We plotted on Fig. 4 the theoretical average attenuation at the end of the excitation period, as a function of $T_e$, for two different diffusion coefficients. The results obtained confirm that diffusion losses should be considerably reduced when using the multi-echo excitation scheme. For example, the simulated intensity losses are 72% for $T_e = 180$ ms with the two-pulse encoding scheme with 0.011 T m$^{-1}$ gradients applied to the ethyl acetate sample. For $n = 3$ with the same $T_e$, they should be reduced to only 22%. However, the multi-echo scheme suffers from drawbacks [12] which reduce its efficiency, and should be optimized in later works.

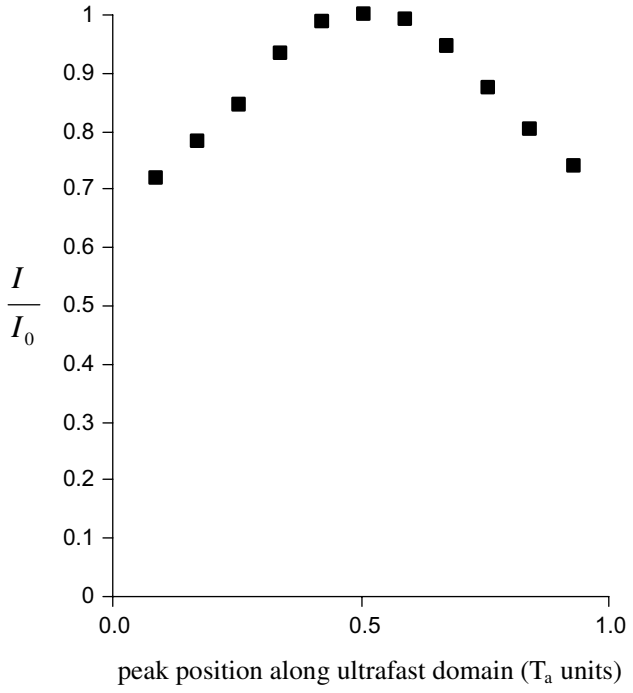


Fig. 5. Intensity losses (average values for three successive experiments) depending on the echo position, for the ethyl acetate singlet on an ultrafast $J$-resolved spectrum acquired with the following parameters: $G_e = 0.032$ T m$^{-1}$, $T_e = 60$ ms, $G_a = 0.047$ T m$^{-1}$ and $T_a = 6.9$ ms. Peak position was modified by slight adjustments of the $G_c$ gradient prior to acquisition. Excitation frequency was set on the relevant signal.

### 2.2. Sensitivity losses during acquisition period

It is also interesting to consider possible diffusion losses during the acquisition period. In particular, for our ultrafast $J$-resolved pulse sequence, the duration $T_a$ of acquisition gradients is not negligible and diffusion losses may occur. To evaluate it, we plotted ethyl acetate singlet 2D peak intensity as a function of its position along the ultrafast $k/v_1$ domain (Fig. 5) 8. Peak position was adjusted by a slight modification of the purge gradient $G_c$ placed just before acquisition. It can be observed that the peak intensity is modulated by its position along the ultrafast domain. It is maximal when the peak is set in the middle of the acquisition window, whereas the minimum value (approximately 70% of maximum intensity) is reached on the edges of ultrafast domain.

In order to make sure that the position-dependent sensitivity losses did not come from the encoding process, we also observed the singlet peak on the first echo as a function on the position. Its intensity did not vary significantly over the $k/v_1$ range contrary to the 2D peak intensity, which proves that the corresponding losses are due to the acquisition process. Moreover, it also shows that the slight adjustments of $G_c$ gradient amplitude, which were necessary to vary the singlet position, do not significantly affect sensitivity.

In order to characterize diffusion effects during the acquisition process, we applied Eq. (1) to our EPI-based $J$-resolved detection scheme. To perform this calculation it should be kept in mind that this scheme leads to two interleaved datasets, consequently two echoes in the same dataset are separated by a $2{\cdot}T_a$ duration. Neglecting the duration of the 180° hard pulses, it can be shown that the intensity decrease between two successive echoes in the same dataset is given by

$$\frac{I_{n+1}}{I_n} = \exp(-b_{acq} \cdot D) \tag{7}$$

where $D$ is the diffusion coefficient, and where $I_{n+1}$ and $I_n$ the relative intensities of the two successive echoes. The diffusion parameter $b_{acq}$ is given by

$$b_{acq} = \frac{2}{3}\gamma^2 G_a^2 \left(\tau^3 + (T_a - \tau)^3\right) \tag{8}$$

where $G_a$ is the amplitude of the acquisition gradient and where $\tau \in [0; T_a]$ is the time when the signal is refocused, *i.e.* the position of the echo along the ultrafast domain. Starting from these equations, we simulated sensitivity losses in the course of the whole ultrafast $J$-resolved acquisition process. The results are plotted in Fig. 6 for the odd dataset of a 64-gradient acquisition, with gradient parameters and diffusion coefficients corresponding to the experimental conditions of Fig. 5. Transverse relaxation was not considered in this model, as it affects all echo positions in a similar way. The simulated curve confirms that the signal decreases much faster when the echo is placed on the

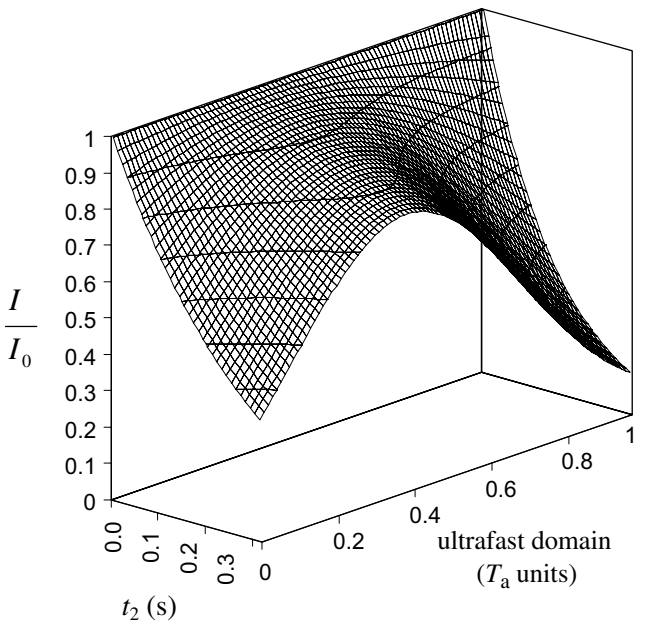


Fig. 6. Simulation of sensitivity losses due to molecular diffusion during an ultrafast *J*-resolved acquisition, with the following parameters: diffusion coefficient $D = 1.0\ 10^{-9}\ m^2\ s^{-1}$, 32 acquisition gradient pairs with $T_a = 6.9$ ms and $G_a = 0.047\ T\ m^{-1}$. Only the dataset corresponding to odd acquisition gradients is represented. Transverse relaxation was not considered in this model.

edges of the ultrafast domain. This faster exponential decay, which comes in addition to transverse relaxation, leads to a more important line broadening and consequently to a non-uniform signal-to-noise decrease depending on the position of the echo peak.

These results show the influence of diffusion effects during *J*-resolved ultrafast acquisition. An important consequence will be the difficulty to perform accurate quantitative measurements with such an acquisition scheme, as all signals in a given sample will not be affected by diffusion in the same manner. A solution could be to perform several ultrafast experiments while successively placing relevant signals in the centre of the ultrafast domain. However, it must be noticed that diffusion effects during acquisition are specific to the *J*-resolved detection scheme, as it uses long acquisition gradients (typically a few ms). Other ultrafast 2D-pulse sequences require shorter acquisition gradients because a bigger spectral width is usually observed in the conventional dimension. Simulations performed with $T_a = 200\ \mu s$ (typical value for homonuclear ultrafast experiments) show that molecular diffusion effects during acquisition are almost non-existent in this case.

In most ultrafast pulse sequences, a mixing period is present between excitation and detection periods. However, this mixing period is the same as the one used in conventional experiments. Consequently, the expression of diffusion or transverse relaxation effects during this period remains the same as the ones obtained with the conventional pulse sequence. Moreover, diffusion losses during the acquisition period are not affected by this mixing period, as they only depend on the acquisition gradient parameters.

## 3. Conclusions

The theoretical and experimental results mentioned in this paper highlight the influence of molecular diffusion on single-scan experiments. Its effects during encoding phase are general to all ultrafast pulse sequences, whereas acquisition diffusion effects are only significant in the *J*-resolved case. It is also shown that homonuclear *J*-couplings have no influence on sensitivity, and that chemical shift offset effects are not significant.

Finally, diffusion effects should be reduced as much as possible by employing weak excitation gradients and also by reducing the diffusion coefficient. This can be achieved by working in a viscous solvent (*e.g.* DMSO) at the lowest temperature possible. Our new multi-echo encoding scheme could also provide a solution to limit diffusion effects. Later works will consider the optimization of this encoding scheme, in particular by optimizing chirp pulse adiabaticity [15].

The limitation of molecular diffusion effects makes it possible to use higher $T_e$ values, thus increasing resolution in the ultrafast dimension. Optimized ultrafast 2D experiments could then replace conventional techniques in a wide range of applications, provided that sufficient S/N is available. Applications in various magnetic resonance domains are expected, from ultrafast *in vivo* spectroscopy to ultrafast *n*D NMR enhanced by Dynamic Nuclear Polarization (DNP) [16].

## 4. Experimental

In order to obtain a 100-mmol $L^{-1}$ solution, 9.8 μL of ethyl acetate, purchased from Rectapur, were dissolved in 1 mL of DMSO-$d_6$. After homogenization, the sample was filtered and analyzed in a 5-mm tube.

NMR spectra were recorded at 303 K on a Bruker Avance 500 DRX spectrometer, at a frequency of 500.13 MHz with a triple resonance TBI probe including *z*-axis gradient. Transverse relaxation times were measured using a classical Carr–Purcell–Meiboom–Gill (CPMG) pulse sequence [17]. Diffusion coefficients were measured using a Pulsed Gradient Spin Echo experiment (PGSE) [13] with various gradient amplitudes ranging from 0 to 0.31 $T\ m^{-1}$.

The ultrafast 2D *J*-resolved spectrum presented on Fig. 1 was obtained with 0.011 $T\ m^{-1}$ excitation gradients and 30 ms Wurst-8 pulses [18] with a sweep range of 9.4 kHz. The same parameters were used for the experiments presented in Fig. 2, but the chirp pulse duration was modified to reach the desired $T_e$ value. For the experiments presented in Fig. 5, 0.032 $T\ m^{-1}$ excitation gradients were used together with 30 ms Wurst-8 pulses with a sweep range of 28.3 kHz.

The $J$-resolved detection block was formed of 64 detection gradients of duration $T_a = 6.9$ ms each. The acquisition gradient amplitude $G_a$ was $0.047\ \mathrm{T\ m^{-1}}$ for experiments in Figs. 1 and 5, and $0.097\ \mathrm{T\ m^{-1}}$ for experiments in Fig. 2. For each experiment, the gradient $G_c$ was set to adjust the echoes at the desired position.

All spectra were processed in the same way: zero-filling once and shifted sine squared apodization function in $v_2$ dimension. All spectra were analysed using the Bruker program Topspin 2.0. Peak intensities were determined on 2D sum projections along the ultrafast axis. The specific processing for ultrafast spectra was performed using our home-written routine in Topspin.

## Acknowledgments

The authors acknowledge Prof. Lucio Frydman for fruitful discussions on ultrafast NMR experiments. We also thank Michel Giraudeau for linguistic assistance.

## Appendix A. Calculation of diffusion factors in ultrafast experiments

The diffusion factors given in Eqs. (3) and (4) can be calculated by considering the model described by Canet in Ref. [19]. When a gradient $g_0$ is applied along the $z$ axis during a duration $t$, the resulting magnetization can be calculated by

$$M(z,t) = \psi(z,t)\exp\left[-(2\mathrm{i}\pi v_0 + 1/\mathrm{T}_2)t\right] \tag{A1}$$

In this expression, $\psi(z,t)$ represents the evolution under molecular diffusion effects, and can be studied independently from precession and transverse relaxation effects. According to Canet [19], $\psi(z,t)$ can be obtained by

$$\psi(z,t) = \psi(z,0)\exp\left(-\mathrm{i}\gamma g_0 z t\right)\exp\left(-D\gamma^2 g_0^2 t^3/3\right) \tag{A2}$$

In order to determine diffusion effects in an ultrafast experiment, it is necessary to calculate the attenuation due to diffusion effects when several successive gradients are applied. For $n$ gradients $g_i$ applied during $t_i$, the global attenuation can be obtained by applying Eq. (A2) $n$ times successively:

$$\psi(z,t) = \psi(z,0)\prod_{i=1}^{n}\exp\left(-\mathrm{i}\gamma g_i z t_i\right)\exp\left(-D\gamma^2 g_0^2 t_i^3/3\right) \tag{A3}$$

In the case of ultrafast excitation schemes, it is also necessary to account for successive inversion effects. Consequently, each excitation scheme should be divided in several successive blocks. For Pelupessy's scheme [10], this decomposition depends on the instant $\tau^\pi$ when the first chirp pulse addresses an internal chemical shift $\Omega_1$ at a particular position $z$. When taking into account the effects of gradient inversion and 180° pulses, Eq. (A3) leads to the signal attenuation due to diffusion at the end of the excitation scheme:

$$\begin{aligned}\psi_{\mathrm{Pel}}(\tau^\pi) = \psi_0 &\exp\left[-\mathrm{i}\gamma G_e^\pi z\tau^\pi\right]\exp\left[-D\gamma^2\left(G_e^\pi\right)^2(\tau^\pi)^3/3\right]\\ &\times\exp\left[\mathrm{i}\gamma G_e^\pi z(\delta^\pi-\tau^\pi)\right]\exp\left[-D\gamma^2\left(G_e^\pi\right)^2(\delta^\pi-\tau^\pi)^3/3\right]\\ &\times\exp\left[\mathrm{i}\gamma\left(-G_e^\pi\right)z(\delta^\pi-\tau^\pi)\right]\\ &\times\exp\left[-D\gamma^2\left(-G_e^\pi\right)^2(\delta^\pi-\tau^\pi)^3/3\right]\\ &\times\exp\left[-\mathrm{i}\gamma\left(-G_e^\pi\right)z\tau^\pi\right]\\ &\times\exp\left[-D\gamma^2\left(-G_e^\pi\right)^2(\delta^\pi-\tau^\pi)^3/3\right]\end{aligned} \tag{A4}$$

which can be easily simplified by

$$\psi_{\mathrm{Pel}}(\tau^\pi) = \psi_0\exp\left[-\frac{2}{3}D\gamma^2\left(G_e^\pi\right)^2\left((\tau^\pi)^3+(\delta^\pi-\tau^\pi)^3\right)\right] \tag{A5}$$

Expression (A5) leads to the diffusion factor $b_{Pel}$ given in Eq. (3). A similar analysis can be carried out for Tal's scheme with inverted gradient [8,9]. When both gradients have the same amplitude ($G_e^\pi = -G_e^{\pi/2}$), Eq. (7) in Ref. [8] leads to $\delta^\pi = -\delta^{\pi/2}/2$. Moreover, we assume that the spoiler gradient after excitation has the same amplitude as the excitation gradients and is applied during $\delta^\pi$. If $\tau^{\pi/2}$ (Eq. (5)) is the instant when the 90° chirp pulse addresses an internal chemical shift $\Omega_1$ at a particular position $z$, the attenuation due to diffusion at the end of the excitation scheme is given by

$$\begin{aligned}\psi_{\mathrm{Tal}}^{\mathrm{inv}}(\tau^{\pi/2}) = \psi_0\exp\Bigg[-\frac{1}{3}D\gamma^2(G_e^{\pi/2})^2\Bigg(&\left(\delta^{\pi/2}-\tau^{\pi/2}\right)^3\\ &+\left(\frac{\delta^{\pi/2}}{2}-\frac{\tau^{\pi/2}}{2}\right)^3+\left(\frac{\tau^{\pi/2}}{2}\right)^3+\left(\frac{\delta^{\pi/2}}{2}\right)^3\Bigg)\Bigg]\end{aligned} \tag{A6}$$

## References

[1] W.P. Aue, E. Bartholdi, R.R. Ernst, Two-dimensional spectroscopy. Application to nuclear magnetic resonance, J. Chem. Phys. 64 (1976) 2229–2246.
[2] J. Jeener, Lecture presented at Ampere International Summer School II, Basko Polje, Yugoslavia, September 1971.
[3] L. Frydman, A. Lupulescu, T. Scherf, Principles and features of single-scan two-dimensional NMR spectroscopy, J. Am. Chem. Soc. 125 (2003) 9204–9217.
[4] L. Frydman, T. Scherf, A. Lupulescu, The acquisition of multidimensional NMR spectra within a single scan, Proc. Natl. Acad. Sci. USA 99 (2002) 15858–15862.
[5] P. Mansfield, Spatial mapping of the chemical shift in NMR, Magn. Reson. Med. 1 (1984) 370–386.
[6] Y. Shrot, B. Shapira, L. Frydman, Ultrafast 2D NMR spectroscopy using a continuous spatial encoding of the spin interactions, J. Magn. Reson. 171 (2004) 163–170.
[7] W.P. Aue, J. Karhan, R.R. Ernst, Homonuclear broad band decoupling and two-dimensional $J$-resolved NMR spectroscopy, J. Chem. Phys. 64 (1976) 4226–4227.
[8] A. Tal, B. Shapira, L. Frydman, A continuous phase-modulated approach to spatial encoding in ultrafast 2D NMR spectroscopy, J. Magn. Reson. 176 (2005) 107–114.
[9] N.S. Andersen, W. Köckenberger, A simple approach for phase-modulated single-scan 2D NMR spectroscopy, Magn. Reson. Chem. 43 (2005) 791–794.

[10] P. Pelupessy, Adiabatic single scan two-dimensional NMR spectroscopy, J. Am. Chem. Soc. 125 (2003) 12345–12350.
[11] P. Giraudeau, S. Akoka, A new detection scheme for ultrafast *J*-resolved spectroscopy, J. Magn. Reson. 186 (2007) 352–357.
[12] P. Giraudeau, S. Akoka, Resolution and sensitivity aspects of ultrafast *J*-resolved 2D NMR spectra, J. Magn. Reson. 190 (2008) 339–345.
[13] T.L. James, G.G. McDonald, Measurement of the self-diffusion coefficient for each compound in a complex system using pulsed-gradient Fourier transform NMR, J. Magn. Reson. 11 (1973) 58–61.
[14] P. Mutzenhardt, F. Guenneau, D. Canet, A procedure for obtaining pure absorption 2D J-spectra: application to quantitative fully J-decoupled homonuclear NMR spectra, J. Magn. Reson. 141 (1999) 312–321.
[15] E. Tenailleau, S. Akoka, Adiabatic $^{1}$H decoupling scheme for very accurate intensity measurements in $^{13}$C NMR, J. Magn. Reson. 185 (2007) 50–58.
[16] L. Frydman, D. Blazina, Ultrafast two-dimensional nuclear magnetic resonance spectroscopy of hyperpolarized solutions, Nat. Phys. 3 (2007) 415–419.
[17] S. Meiboom, D. Gill, Modified spin–echo method for measuring nuclear relaxation times, Rev. Sci. Instrum. 29 (1958) 688–691.
[18] E. Kupce, R. Freeman, Adiabatic pulses for wideband inversion and broadband decoupling, J. Magn. Reson. A 115 (1995) 273–276.
[19] D. Canet, J.-C. Boubel, E. Canet Soulas, La RMN, Concepts, méthodes et applications, Dunod ed., Paris, 2002, Appendix A4-1.